RadioGraphics

MR Imaging Features of Vaginal Malignancies[1]

Jyoti H. Parikh, FRCR • Desmond P. J. Barton, FRCS • Thomas E. J. Ind, FRCS • S. Aslam Sohaib, FRCR

CME FEATURE

See accompanying test at http://www.rsna.org/education/rg_cme.html

LEARNING OBJECTIVES FOR TEST 1

After reading this article and taking the test, the reader will be able to:

- Discuss the patterns and extent of disease in squamous cell primary vaginal carcinoma.
- List the MR imaging features of the histologic subtypes of nonsquamous primary vaginal carcinoma.
- Describe the disease patterns and MR imaging features of gynecologic and nongynecologic vaginal metastases.

TEACHING POINTS

See last page

Primary vaginal malignancies are rare, accounting for only 1%–2% of all gynecologic malignancies. Squamous cell carcinoma makes up about 85% of primary vaginal malignancies. This tumor characteristically arises from the posterior wall of the upper third of the vagina. The main patterns of disease are an ulcerating or fungating mass or an annular constricting lesion. At magnetic resonance (MR) imaging, squamous cell carcinoma has intermediate signal intensity on T2-weighted images and low signal intensity on T1-weighted images. The tumors that account for the remaining 15% of primary vaginal malignancies are adenocarcinoma, melanoma, and sarcomas. The signal intensity characteristics on MR images correlate with the histologic subtypes and reflect the MR imaging appearances of these histologic subtypes elsewhere in the body. Secondary malignancy of the vagina is far more frequent than primary vaginal malignancy. Most vaginal metastases occur by means of direct local spread from the cervix, uterus, or rectum. The MR imaging appearances of these metastases reflect the MR imaging appearances of the primary tumor.

Abbreviations: FIGO = International Federation of Gynecology and Obstetrics, STIR = short inversion time inversion-recovery

RadioGraphics 2008; 28:49–63 • **Published online** 10.1148/rg.281075065 • **Content Codes:** GU MR OB OI

[1]From the Departments of Radiology (J.H.P., S.A.S.) and Surgical Gynecologic Oncology (D.P.J.B., T.E.J.I.), Royal Marsden Hospital NHS Foundation Trust, Fulham Road, London SW3 6JJ, United Kingdom. Presented as an education exhibit at the 2006 RSNA Annual Meeting. Received April 4, 2007; revision requested May 7 and received July 5; accepted July 24. All authors have no financial relationships to disclose. **Address correspondence to** S.A.S. (e-mail: *aslam.sohaib@rmh.nhs.uk*).

Table 1
FIGO Staging Classification for Vaginal Carcinoma

FIGO Stage	Description	TNM Category
0	Carcinoma in situ	Tis
I	Tumor confined to the vagina	T1
II	Tumor invades paravaginal tissues but not the pelvic sidewall	T2
III	Tumor extension to the pelvic sidewall	T3
IVA	Tumor extends beyond the true pelvis and invades the bladder, urethra, or rectum	T4
IVB	Distant metastases	M1

Introduction

Primary vaginal carcinoma is rare, accounting for only 1%–2% of gynecologic malignancies and ranking fifth in frequency behind carcinoma of the ovary, uterus, cervix, and vulva (1). Malignant involvement of the vagina occurs more commonly from metastatic spread, and except for isolated reports of metastases from extragenital cancers (2), the most common cause of metastatic disease is direct local invasion from the female urogenital tract. Therefore, primary vaginal carcinoma should be diagnosed only if other gynecologic malignancies have been excluded. Primary vaginal carcinomas are defined as arising solely from the vagina with no involvement of the external os superiorly or the vulva inferiorly, the importance of this definition lying in the different clinical approaches in the treatment of cervical and vulval carcinoma (3,4).

Teaching Point

The clinical and histopathologic features of primary vaginal malignancies have been well documented (1,5–8). As with all gynecologic malignancies, the staging of vaginal carcinoma uses the International Federation of Gynecology and Obstetrics (FIGO) staging system (Tables 1, 2) and for vaginal cancer is based on the clinical findings, as for cervical cancer. However, magnetic resonance (MR) imaging can provide details not readily assessed at examination under anesthesia. MR imaging is crucial in demonstrating the location of the tumor, parametrial extension, pelvic sidewall involvement, and spread to the bladder or urethra, rectum, and lymph nodes. Furthermore, MR imaging can be of value in depicting pelvic anatomy for surgical and radiation therapy planning.

Teaching Point

MR imaging with its higher soft-tissue contrast than computed tomography (CT) and direct multiplanar imaging performs better than clinical examination alone for assessment of vaginal lesions and has been shown to be useful for evaluating the size, location, and extent of vaginal tumors, demonstrating the degree of lymph node involvement, and preoperative planning (9–12). The histologic diagnosis for vaginal malignancies is often established prior to MR imaging examination because it is relatively easy to perform biopsy for vaginal tumors. However, this may not be the case for all vaginal tumors, particularly nonsquamous tumors, and MR imaging may therefore have a role in determining a route for biopsy.

Table 2
Correlation of TNM Categories with FIGO Stage of Vaginal Carcinoma

FIGO Stage	TNM Categories
0	Tis N0 M0
I	T1 N0 M0
II	T2 N0 M0
III	T1 N1 M0, T2 N1 M0, T3 any N M0
IVA	T4 any N M0
IVB	Any T any N M1

To our knowledge, there is only limited literature with only case reports or small case series describing the MR imaging features of the variety of histologic types of vaginal malignancies. We present a review of primary vaginal malignancies and vaginal metastases and discuss their imaging features with respect to MR imaging.

MR Imaging Technique

Our basic imaging protocol consists of axial T1-weighted and T2-weighted fast spin-echo imaging through the pelvis from the aortic bifurcation to below the vulva. This gives an overview of the whole pelvis and allows assessment of pelvic and inguinal lymphadenopathy. Sagittal T2-weighted fast spin-echo imaging from pelvic sidewall to sidewall allows assessment of vaginal tumor extension to the uterus, bladder, urethra, and rectum. These sequences are supplemented with high-resolution oblique axial (ie, perpendicular to the long axis of the vagina) T2-weighted fast spin-echo imaging (11). This sequence allows detailed assessment of the vaginal tumor and its relation to the paravaginal tissues and thus accurately demonstrates the extent of disease. Vaginal tumors are almost always best seen with this sequence. Coronal T2-weighted images allow evaluation of the

Teaching Point

pelvic sidewall in larger tumors. We do not routinely use intravenous gadolinium contrast material because paravaginal tissue often enhances avidly, thus reducing the conspicuity between the tumor and other structures.

Squamous Cell Primary Vaginal Carcinoma

Clinical Features

Squamous cell carcinoma accounts for 85%–87% of primary vaginal cancers, occurring predominantly in postmenopausal women (peak age 60 years) who usually present with painless vaginal bleeding (65%–80%), abnormal discharge (30%), urinary symptoms (20%), pelvic pain (15%–30%), or a feeling of a mass within the vagina (10%) or are asymptomatic (10%–27%) (6). Squamous carcinoma of the vagina is associated with human papilloma virus and vaginal intraepithelial neoplasia, and up to 30% of patients have a history of intraepithelial or invasive carcinoma of the cervix or vulva. Up to 10% of patients have a history of vaginal radiation therapy for cervical carcinoma (13).

Primary vaginal squamous cell carcinoma most commonly occurs in the upper third of the vagina on the posterior wall (8). It tends to spread early, by direct invasion of the bladder and urethra anteriorly and the rectum posteriorly. One-third of patients have pelvic or groin lymph node involvement at diagnosis owing to early spread through the blood and lymphatics (14).

Treatment and Prognosis

Treatment is variable, with superficial carcinomas at the vaginal vault or in the posterior fornix being treated with radical vaginectomy (with radical hysterectomy if the uterus is present) and pelvic lymphadenectomy (15). Tumors in the lower third are treated with radical excision and inguinal lymphadenectomy. Deeply infiltrative tumors are best treated with radiation therapy, which offers vaginal preservation and preservation of the bladder and anal sphincters. Various chemotherapy regimens are used to treat metastatic disease. Primary vaginal carcinoma has a 5-year survival of about 80% for stage I or II disease, falling to 20% for stage III or IV tumors (9).

Most recurrences occur within a year and have a poorer prognosis. Lesions of the upper third tend to recur locally; those of the lower third tend to recur at distant sites and the pelvic sidewall.

MR Imaging Appearances

Macroscopically, the most common patterns of presentation of primary vaginal squamous cell carcinoma are an ulcerating lesion (50%), a fungating mass (30%), or an annular constricting mass (20%) (16). The pattern of appearance of disease at MR imaging correlates well with this macroscopic pattern of disease, with tumors appearing as an ill-defined, irregular, diffuse mass (the ulcerating pattern of disease); a well-defined lobulated mass (the fungating pattern of disease); or a circumferential thickening (the annular constricting pattern of disease). The exophytic tumors are associated with a significantly better prognosis than the infiltrative ones (16–18). This may be due to the fact that exophytic tumors tend to grow more superficially, while ulcerative ones are more likely to invade subvaginal tissue and therefore metastasize (15,17).

At MR imaging, squamous cell carcinomas are best seen with T2-weighted sequences. They appear as a mass of homogeneous intermediate signal intensity (higher than that of muscle, lower than that of fat) that can be appreciated as separate from the low signal intensity of the vaginal wall; therefore, its location and extent can be accurately assessed with high-resolution T2-weighted imaging (9). Some tumors may contain high-signal-intensity foci, and this should raise the possibility of the tumor being a poorly differentiated squamous cell carcinoma, with the high-signal-intensity foci representing tumoral necrosis (19). If this appearance is seen, then an adenosquamous carcinoma, mucinous adenocarcinoma, or metastases from the cervix or uterus should be considered (20).

At T1-weighted imaging, squamous cell carcinoma appears as an isointense to muscle lesion, and its presence can be appreciated only when the lesion is large enough to alter the vaginal contour.

MR imaging is used for evaluation of tumor extent and detection of nodal metastasis. For evaluation of nodal disease, either CT or MR imaging can be used, but for evaluation of local tumor extent, MR imaging is the preferred modality due to its superior soft-tissue contrast resolution. Stage I tumors, that is, those limited to the vaginal mucosa, appear as a mass or plaque of tissue of intermediate signal intensity on T2-weighted images, expanding and filling the vagina but with preservation of the low signal intensity of the outer vaginal muscularis layer. However, in stage II, tumor extension into the paravaginal tissue is well delineated on MR images by loss of the low

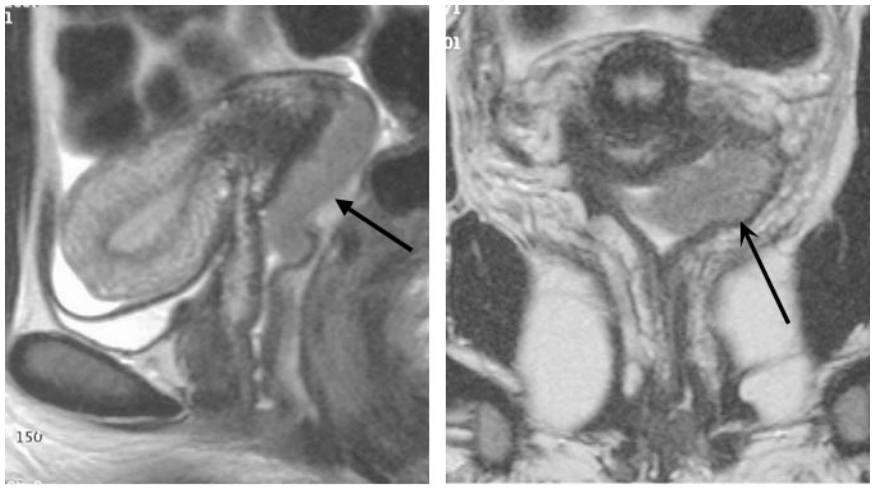

a. b.

Figure 1. FIGO stage II squamous cell carcinoma in a 29-year-old patient with a fungating vaginal mass. **(a)** Sagittal T2-weighted MR image shows a diffuse, lobulated, 4 × 1.4 × 5.5-cm mass arising from the posterior wall of the upper vagina. The mass has intermediate signal intensity relative to that of muscle. Strands of the intermediate-signal-intensity tumor extend through the low-signal-intensity rim of the vaginal muscularis and infiltrate the rectovaginal fat plane (arrow). **(b)** Coronal T2-weighted MR image shows that the mass abuts but does not invade the left lateral vaginal fornix (arrow).

signal intensity of the vaginal muscularis layer (21) (Fig 1).

In stage III, tumor extends laterally to the pelvic sidewall, which is best seen on the axial and coronal images. Tumor involvement of sidewall musculature is best seen on T2-weighted images. The low signal intensity of the sidewall muscle and pelvic floor contrasts with the intermediate signal intensity of the tumor (22) (Fig 2).

Stage IVA disease manifests as invasion of the *mucosa* of the bladder or rectum. The presence of bullous edema is not sufficient evidence to classify a tumor as stage IVA. Invasion through the low signal intensity of the bladder or rectal wall is best evaluated on T2-weighted images. In addition to loss of the intervening vesicovaginal fat plane or the rectovaginal septum, tumor infiltration of the bladder or rectum is seen (Fig 3) (23). In stage IVB, disease spreads beyond the pelvis and may involve the peritoneum and small or large bowel loops (Fig 4). The most common sites of distant metastases are the lung, liver, and bone.

MR imaging may be used in evaluating complications of the disease and treatment, such as vesicovaginal or rectovaginal fistulas. This is best demonstrated on sagittal or axial sections from high-resolution T2-weighted or short inversion time inversion-recovery (STIR) imaging. MR imaging is also valuable in differentiating between tumor and scar tissue in patients in whom recurrent disease is suspected. This can be difficult, but scar tissue appears as low signal intensity, whereas tumor demonstrates intermediate to high signal intensity on T2-weighted images. Furthermore, tumor may have a masslike appearance. Enhancement after intravenous administration of gadolinium contrast material may also help, but inflammatory change in scar tissue may also enhance and require a biopsy (24).

Nonsquamous Primary Vaginal Carcinomas

Non–squamous cell carcinomas account for 15% of all primary vaginal carcinomas. They manifest at an earlier stage, in a younger subset of patients, and have better prognostic outcomes than primary squamous vaginal carcinoma (19,25,26). They are more likely to recur than squamous cell carcinomas. There is little data available on the time frame for recurrence of nonsquamous primary vaginal carcinomas, with a wide range documented from between 1 and 7 years from manifestation of the primary tumor.

Adenocarcinoma

Adenocarcinomas account for 9% of primary vaginal carcinomas (13). They typically occur in younger women aged 14–21 years (peak age, 19 years). In these younger women, primary vaginal adenocarcinoma is thought to arise from areas of

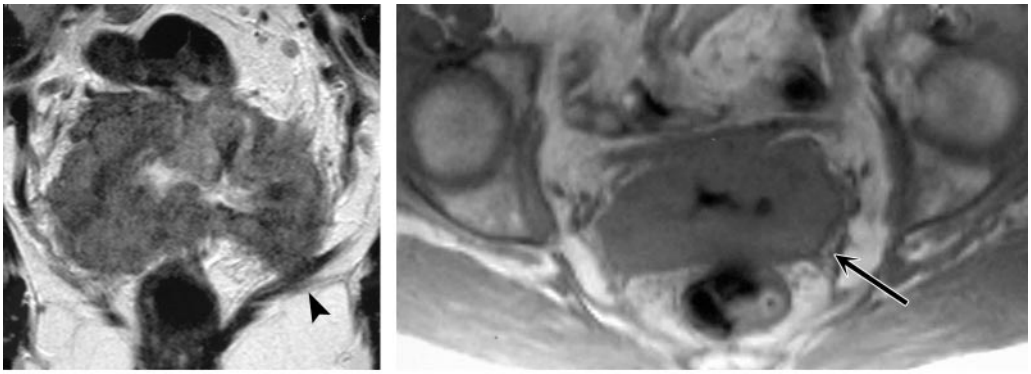

a. b.

Figure 2. FIGO stage III squamous cell carcinoma in a 73-year-old patient with postmenopausal bleeding. **(a)** Coronal T2-weighted MR image shows irregular circumferential thickening of the vaginal vault that has intermediate signal intensity and extends to the left levator sling (arrowhead). **(b)** Axial T1-weighted MR image shows that the mass is hypointense relative to fat and isointense relative to muscle. There is extension to the parametrium (arrow).

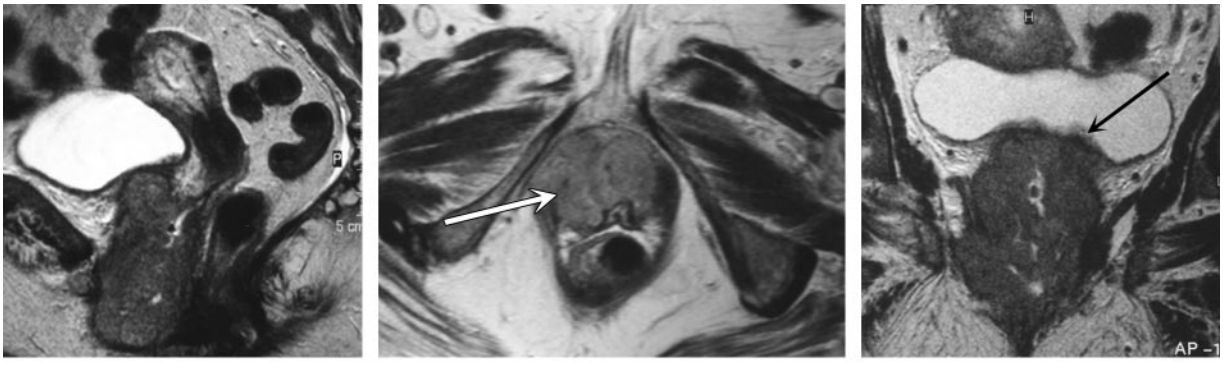

a. b. c.

Figure 3. FIGO stage IVA squamous cell carcinoma in an 84-year-old patient with postmenopausal bleeding. **(a)** Sagittal T2-weighted MR image shows an irregular, 6 × 4 × 9-cm, intermediate-signal-intensity mass that arises from the anterior and right lateral walls of the vagina and extends from the vault to the introitus. **(b)** Axial T2-weighted MR image shows that the mass (arrow) extends laterally to the right and left levator ani muscles. **(c)** Coronal T2-weighted MR image shows invasion of the base of the bladder (arrow).

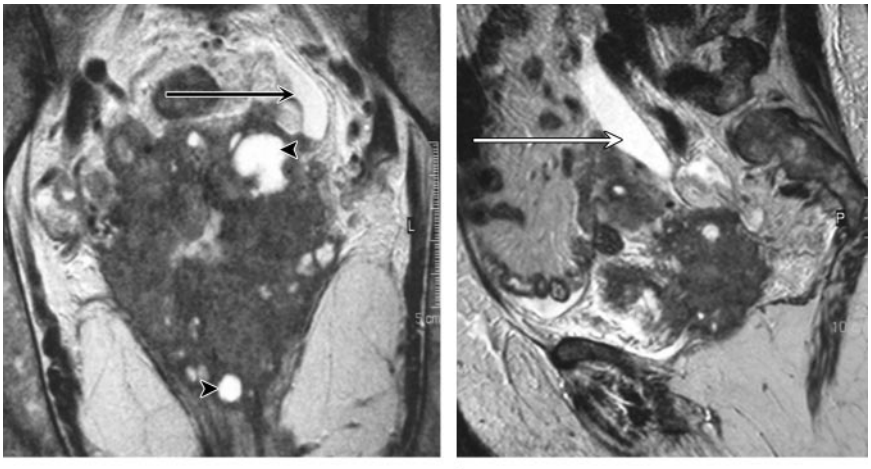

a. b.

Figure 4. FIGO stage IVB squamous cell carcinoma in a 70-year-old patient with postmenopausal bleeding. **(a)** Coronal T2-weighted image shows a bulky, diffuse, irregular, 8 × 9 × 11-cm mass of low to intermediate signal intensity arising from the vagina. The tumor extends to the pelvic sidewall and bladder and obstructs the left distal ureter (arrow). It contains multifocal areas of high signal intensity (arrowheads) that may represent fluid or mucin from tumoral necrosis. **(b)** Sagittal T2-weighted image shows that the mass infiltrates the sigmoid colon (arrow).

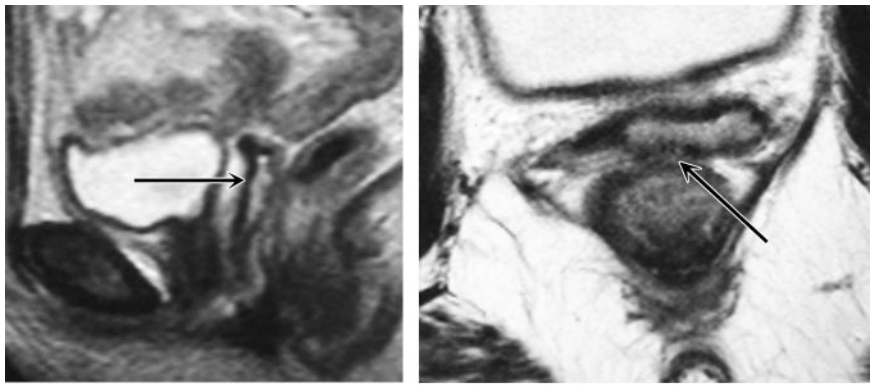

a. b.

Figure 5. FIGO stage I adenocarcinoma in a 62-year-old patient with a history of vaginal adenocarcinoma treated with chemotherapy and radiation therapy who presented with postmenopausal bleeding. The patient had no history of exposure to diethylstilbestrol; adenocarcinoma in this age group is thought to be a clear cell histologic subtype. **(a)** Sagittal T2-weighted MR image shows a homogeneous, 3 × 1 × 3.5-cm, high-signal-intensity plaque arising from the upper posterior wall of the vagina (arrow). **(b)** Axial T2-weighted MR image shows no loss of the rectovaginal fat plane (arrow).

vaginal adenosis but may also arise in foci of endometriosis, wolffian rest remnants, and periurethral glands (26). Of those women presenting at a younger age, two-thirds have a history of exposure to diethylstilbestrol in utero, dating from the 1950s to the 1970s when diethylstilbestrol was given to mothers at risk for miscarriage (7,25). The pattern of disease seen in older women has been described in the gynecologic oncology literature as primary vaginal clear cell adenocarcinoma that is most likely of müllerian origin (27).

Primary vaginal adenocarcinoma occurs mainly in the upper third and anterior wall of the vagina, although there have been case reports in the pathology literature of tumor arising from the posterior wall (28). Macroscopically, primary vaginal adenocarcinoma appears as a polypoid, papillary, plaquelike, or ulcerated lesion (29). The appearances of primary vaginal adenocarcinoma at MR imaging have been described as a bulky lobulated vaginal mass or diffuse circumferential thickening of the vaginal wall (25,30), appearances that are compatible with a macroscopic polypoid or papillary lesion. Primary vaginal adenocarcinoma appears homogeneously hyperintense on T2-weighted images and isointense to muscle on T1-weighted images (23,25,30,31) (Fig 5). Owing to the intrinsic high signal intensity of this epithelial tumor with T2-weighted sequences, MR imaging can demonstrate the low signal intensity of the vaginal wall and can therefore accurately demonstrate invasion into the paravaginal tissues (30).

Melanoma

Primary vaginal malignant melanoma accounts for less than 0.5%–2% of melanomas in women and less than 3% of all vaginal malignancies (31), vulval melanomas being more common (7). Malignant melanoma of the vagina is a disease of postmenopausal women, with 75% of women being over 50 years of age (32). Primary vaginal melanoma may arise anywhere in the vagina with a predilection for the lower third (7) and for the anterior and lateral walls (31). Macroscopically, primary vaginal melanoma appears as a brownish to black, soft mucosal or submucosal nodular, pedunculated papillary or lobulated mass (27). Ulceration and necrosis are often present, mimicking squamous cell carcinoma (27,33). Malignant melanoma is usually pigmented but may be devoid of pigment (amelanotic melanoma) and can contain both pigmented and nonpigmented lesions in a zosteriform pattern (34). Amelanotic melanoma accounts for only 5% of primary vaginal melanomas (27).

MR imaging features of melanomas in the head have been widely investigated and consist of high signal intensity on T1-weighted images and low signal intensity on T2-weighted images (35), this appearance being attributed to the paramagnetic effects of melanin and methemoglobin from intratumoral necrosis or hemorrhage. Melanin shortens T1 and T2 relaxation times, resulting in high signal on T1-weighted images and low signal on T2-weighted images. Although reported, MR imaging features of vaginal melanomas are few in number and differ somewhat from typical MR imaging findings in the head, varying according to the melanin concentration and presence of hemorrhage.

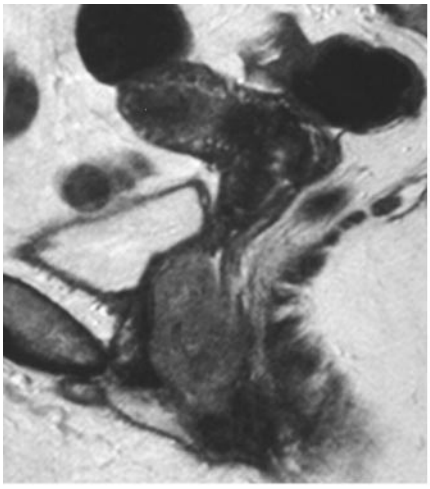

6a.

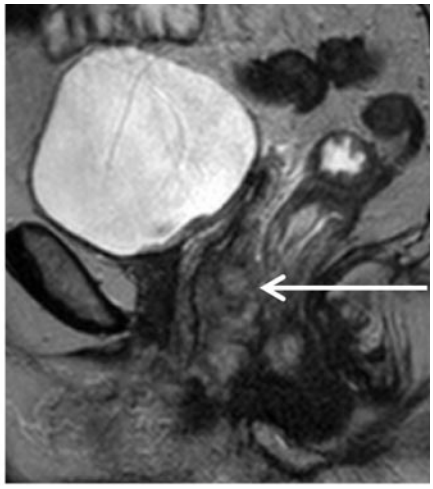

7a.

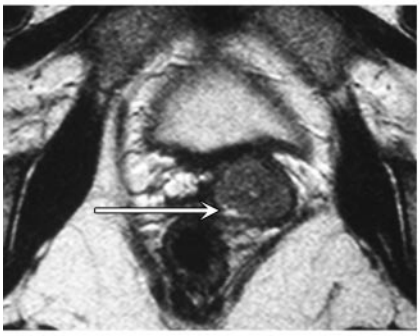

6b.

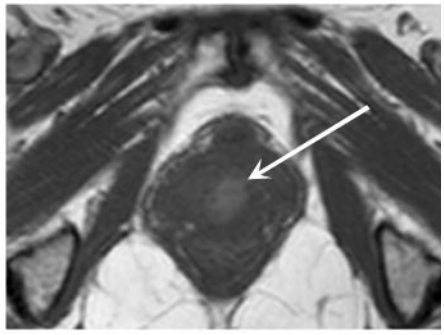

7b.

Figures 6, 7. **(6)** FIGO stage I melanoma in a 60-year-old patient with postmenopausal bleeding. **(a)** Sagittal T2-weighted MR image shows a 4.5 × 3 × 2.6-cm, lobulated, homogeneous mass of intermediate signal intensity, which arises from the anterior and posterior walls of the vagina and extends its entire length from the vault to the introitus. **(b)** Axial T2-weighted MR image shows that the low-signal-intensity rim of the vaginal wall is intact (arrow). **(7)** FIGO stage IVA melanoma in a 70-year-old patient with postmenopausal bleeding. **(a)** Sagittal T2-weighted MR image shows a bulky, heterogeneous, 3.7 × 2.5 × 2.8-cm mass of intermediate signal intensity, which arises from the lower third of the posterior wall of the vagina. The mass extends posteriorly to the anterior wall of the rectum (arrow) and laterally to the levator ani muscles. **(b)** Axial T1-weighted MR image shows that the predominantly low-signal-intensity mass has a center of slightly higher signal intensity (arrow), a finding suggestive of melanin content.

For this reason, some primary vaginal melanomas appear as typical high-signal-intensity lesions on T1-weighted images with low signal intensity on T2-weighted images (36,37) (Fig 6) or as intermediate to high signal intensity on T1-weighted images and intermediate to high signal intensity on T2-weighted images (32,34,36,37) (Fig 7), the signal intensity of most tumors on T2-weighted images being higher than that of the adjacent muscles on T1-weighted images. Amelanotic melanomas appear as low signal intensity on T1-weighted images and intermediate to high signal intensity on T2-weighted images (7). Therefore, the absence of high signal intensity on T1-weighted images should not preclude the diagnosis of malignant melanoma (10,36). Melanomas are much more clearly demonstrated on fat-suppressed images with brighter signal as the dynamic range becomes narrower, allowing detection of subtle differences (38).

Leiomyosarcoma

Sarcomas account for less than 3% of primary vaginal malignancies. Primary vaginal leiomyosarcoma, a tumor of smooth muscle origin, is the most common vaginal soft-tissue sarcoma in adults (27). It accounts for less than 2% of all primary vaginal cancers, with a wide age range of 25–86 years (39), and may occur after radiation therapy to the genital tract. Primary vaginal leiomyosarcoma is thought to originate from the rectovaginal septum, mainly involving the upper

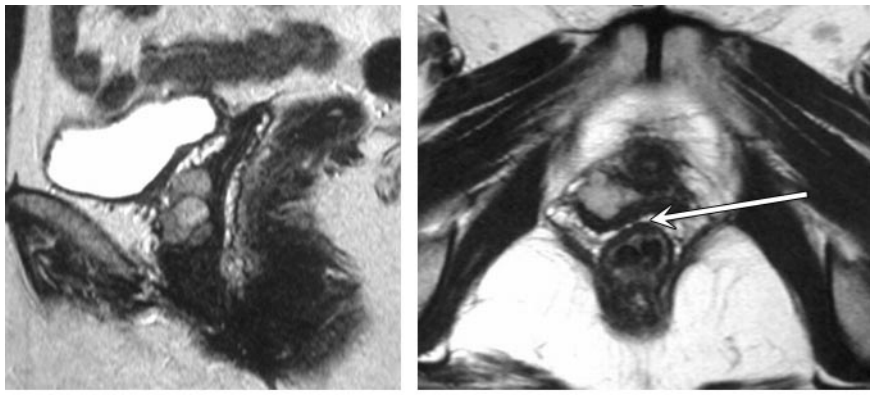

a. b.

Figure 8. FIGO stage II leiomyosarcoma in a 58-year-old patient with a vaginal mass who previously underwent transvaginal excision of a rectovaginal leiomyosarcoma. **(a)** Sagittal T2-weighted MR image shows a 3.5 × 2 × 1.5-cm, lobulated, well-circumscribed, multiseptate mass of intermediate to high signal intensity, which arises from the anterior wall of the upper vagina, invading the paravaginal tissues but not extending to the pelvic sidewall. **(b)** Axial T2-weighted MR image shows the intermediate-signal-intensity lobulated mass arising from the upper anterior wall of the vagina with an intact rectovaginal septum (arrow).

vagina and grossly appearing as a bulky submucosal lesion. The biologic activity of vaginal leiomyosarcoma is similar to that of uterine leiomyosarcoma (27,40).

At MR imaging, primary uterine leiomyosarcomas are described as heterogeneous masslike lesions with areas of high T2-weighted signal intensity corresponding to cystic necrosis in the tumor and pockets of high T1-weighted signal intensity corresponding to acute hemorrhage (41). The limited reports of vaginal leiomyosarcomas suggest that they may have a similar range of appearances on MR images to leiomyosarcoma elsewhere. A case report of the MR imaging features of vaginal metastases from uterine leiomyosarcoma describes an indistinct heterogeneous mass in the vagina with intermediate to high signal intensity on T2-weighted images and low to intermediate signal intensity on T1-weighted images (37). A case report of vaginal leiomyosarcoma describes an irregular, locally infiltrative mass with high signal intensity on T2-weighted images and a heterogeneous appearance with areas of necrosis and hemorrhage (42) (Fig 8).

The first case report referred to (37) describes a case of vaginal metastases from uterine leiomyosarcoma as showing early peripheral enhancement with gadolinium with progressive heterogeneous fill-in of the lesion on delayed images, and the other authors described primary vaginal leiomyosarcomas as showing diffusely heterogeneous enhancement with gadolinium owing to the presence of areas of necrosis or hemorrhage (42), further suggesting that vaginal metastases from uterine leiomyosarcoma and primary vaginal leiomyosarcoma show similar enhancement characteristics with gadolinium on postcontrast MR images. The case in our series also underwent imaging with STIR sequences—to our knowledge, the appearance of primary vaginal leiomyosarcoma with this sequence has not been reported. The tumor showed very high signal intensity on STIR images, similar to the appearance of skeletal metastases from uterine leiomyosarcoma (43).

Spindle Cell Synovial Sarcoma

Primary vaginal synovial cell sarcoma is rarer than primary vaginal leiomyosarcoma. It is an aggressive soft-tissue tumor arising from mesenchymal or epithelial cells. Although the clinical and pathologic features of vaginal synovial sarcoma have been well documented (44,45), our review of the literature revealed that the MR imaging features have not been documented, to our knowledge.

However, the MR imaging features of synovial sarcoma of the extremities are well described (46,47). Such tumors have been described as well-defined ovoid or lobulated masses that cause displacement of adjacent structures rather than invasion. Lesions are hyperintense on T2-weighted images, with larger lesions showing considerable inhomogeneity secondary to necrosis and cystic components and smaller lesions having predominantly homogeneous signal intensity. Lesions appear as heterogeneous signal intensity on T1-weighted images and demonstrate early heterogeneous enhancement with gadolinium contrast material (46).

Our case of primary vaginal synovial sarcoma (Fig 9) showed a similar pattern, appearing as a

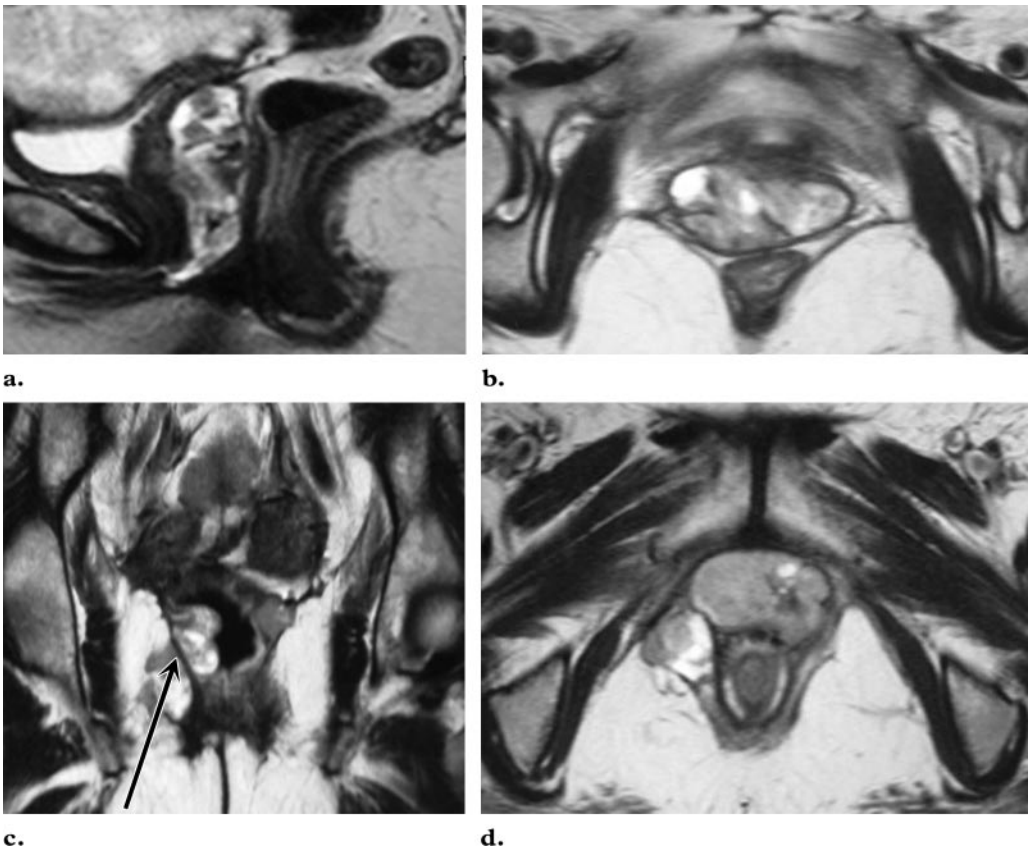

Figure 9. Spindle cell synovial sarcoma in a 50-year-old patient with a history of uterine carcinosarcoma who presented with a vaginal mass. Although the tumor was FIGO stage I at initial imaging **(a, b)**, imaging performed 8 months later showed progression to FIGO stage III **(c, d)**. **(a)** Sagittal T2-weighted MR image shows a well-circumscribed lobulated mass of very high signal intensity that fills the entire length of the vagina, with multifocal areas of low-signal-intensity necrosis within it. **(b)** Axial T2-weighted MR image shows the tumor expanding and filling the vagina with the low-signal-intensity rim of the vaginal wall remaining intact. **(c)** Coronal T2-weighted MR image shows the tumor breaching the right levator sling (arrow) and extending to the right ischioanal fossa. **(d)** Axial T2-weighted MR image shows the tumor extending 180° around the rectum but not invading it. These tumors tend to displace rather than invade adjacent structures.

well-circumscribed very high-signal-intensity mass with focal areas of low signal intensity within it on T2-weighted images (Fig 9a, 9b) and as a heterogeneous intermediate-signal-intensity mass on T1-weighted images. The tumor displaced rather than invaded tissues planes as the disease progressed (Fig 9c, 9d).

Other Primary Vaginal Malignancies

There are other histologic subtypes of adult primary vaginal carcinomas such as paragangliomas and lymphoma, but these subtypes are rare (7,48,49). In children, vaginal sarcoma botryoides (embryonal rhabdomyosarcoma) is a rare aggressive tumor occurring in girls (peak age, 3 years). This appears as a grapelike mass with very high signal intensity on T2-weighted MR images. Vaginal endodermal sinus tumor (yolk sac tumor) is another very rare type of adenocarcinoma, classified as a germ cell tumor with a peak incidence of 10 months.

Lymph Node Involvement

Teaching Point

The lymph node drainage pattern of the vagina is such that lesions of the upper and middle thirds drain to the pelvic obturator nodes, internal and external iliac nodes, and paraaortic nodes and lesions of the lower third drain to the inguinal nodes. Posterior wall lymphatics communicate with rectal lymphatics and drain to the inferior gluteal, sacral, and rectal nodes. Disease progression or lesions involving the whole length of the vagina may involve both the inguinal and iliac nodal groups. This pattern of nodal involvement is reflected in the MR imaging appearances of vaginal malignancies (50).

Vaginal Metastases

Secondary malignancies of the vagina are far more common than primary tumors and account for more than 80% of all vaginal tumors (13).

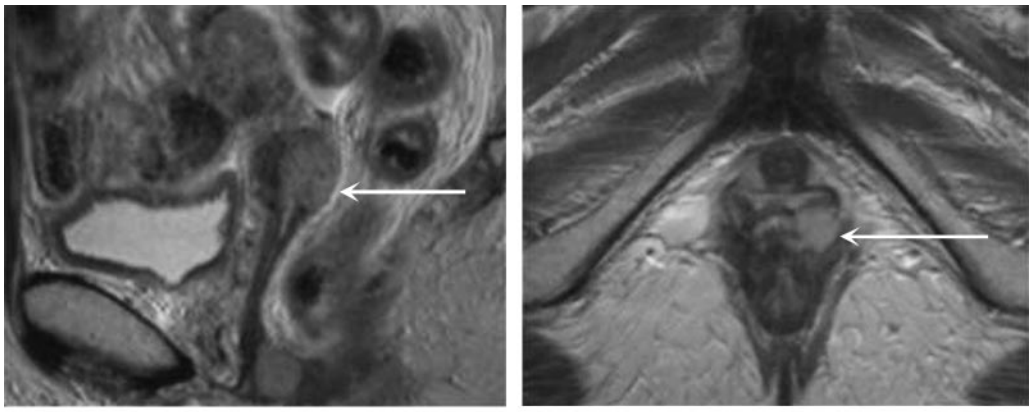

a. b.

Figure 10. Vaginal metastases (skip lesions) in a 63-year-old patient with treated squamous cell carcinoma of the cervix who presented with an irregular mass at the vaginal vault. **(a)** Sagittal T2-weighted MR image shows an ill-defined intermediate-signal-intensity mass in the vaginal vault that bulges posteriorly into the rectovaginal septum (arrow). This is a typical site for recurrence of squamous cell cervical carcinoma. **(b)** Axial T2-weighted MR image shows a second ill-defined intermediate-signal-intensity mass in the lower third of the vagina abutting the left anterolateral wall of the anal canal (arrow). Although this is an uncommon site for metastases from a primary tumor, such skip lesions in the lower third of the vagina are found in recurrent disease.

The majority of vaginal metastases occur through direct contiguous spread from malignancies from adjacent tumors. Remote vaginal metastases may occur through lymphatic or hematogenous spread. The most common malignancies to metastasize to the vagina are ovarian, cervical, endometrial, and rectal cancer. There have been isolated reports of metastases from extragenital cancers, from adenocarcinoma of the colon, breast, pancreas, and small bowel (2).

Seventy-five percent of squamous vaginal metastases arise from the cervix and 14% from the vulva (51,52). Of the vaginal metastases that are adenocarcinomas, 92.5% of lesions in the upper third and anterior wall arise from the upper genital tract, while 90% of lesions in the lower third and posterior wall arise from the gastrointestinal tract (52). Eighty percent of vaginal metastases occur within the first 3 years after the primary tumor, and 67% occur after surgical removal of the primary lesion. Disseminated metastatic disease is frequently present in patients with vaginal metastases and therefore the prognosis is extremely poor. As a general rule, the MR imaging features of metastases to the vagina mimic the MR imaging features of the primary tumor, and T2-weighted MR imaging best delineates the extent of disease within and beyond the vagina.

Teaching Point

Metastases from Gynecologic Malignancies

Cervical cancer commonly involves the vagina, and FIGO staging of cervical cancer includes involvement of the vagina. The proximal two-thirds of the vagina is most commonly invaded. Rarely in more advanced cervical cancer, the distal third of the vagina is affected. Spread to the vagina is by direct contiguous spread. Skip lesions in the vagina may be seen in recurrent cervical cancer (Fig 10), in which case lesions may be seen in the distal vagina. Patterns of involvement of the vagina follow the growth pattern of the primary cervical cancer (eg, as a masslike lesion or as an infiltration along the vaginal wall). The signal intensity of vaginal disease is typically intermediate to high on T2-weighted MR images and low on T1-weighted MR images (Fig 11).

Vaginal involvement in uterine cancer is uncommon and occurs in advanced disease (FIGO stage IIIB uterine cancer). This occurs either with direct extension of tumors from the uterus or from metastatic disease (ie, from tumor seeding from the uterus into the vagina). Therefore, it is important when staging endometrial cancer with MR imaging that the vagina is examined to look for metastatic spread if there is not direct extension of disease. Rarely, endometrial cancer may spread into the peritoneal cavity and involve the peritoneal reflection on the vaginal fornix; however, this is more common in ovarian cancer. Most metastases are endometrial adenocarcino-

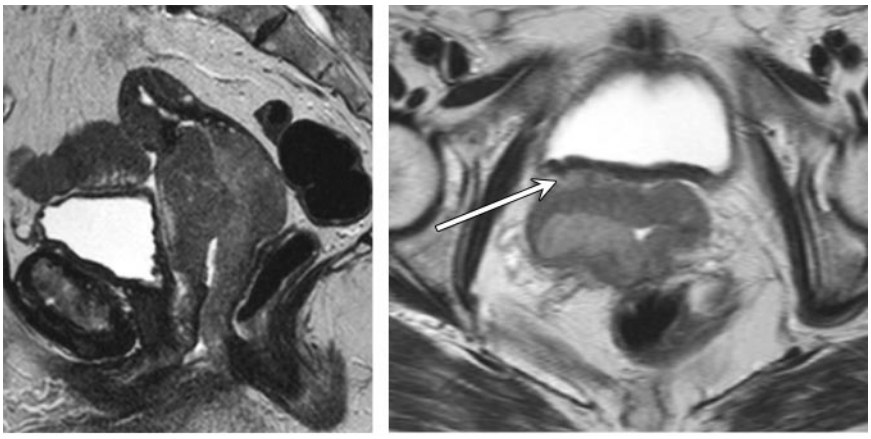

a. b.

Figure 11. Vaginal metastasis from squamous cell carcinoma of the cervix in a 79-year-old patient with a bulky vaginal mass and urinary symptoms. The patient was found to have stage IIIB poorly differentiated squamous cell carcinoma of the cervix. **(a)** Sagittal T2-weighted MR image shows a well-defined, bulky, 6 × 9 × 6-cm mass that arises from the cervix and extends to the lower uterine segment and the lower third of the vagina. **(b)** Axial T2-weighted MR image shows the mass bulging into the posterior wall of the bladder but not invading it (arrow).

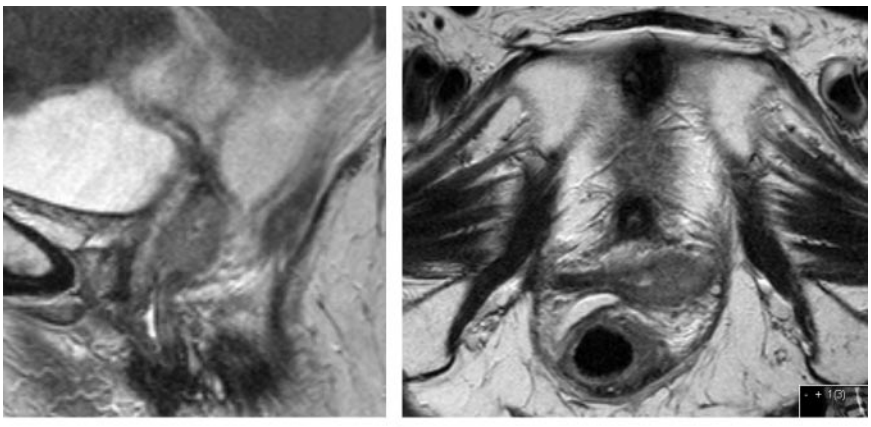

a. b.

Figure 12. Vaginal metastasis in an 83-year-old patient with a history of endometrioid adenocarcinoma of the endometrium who presented with a recurrent mass in the vaginal vault. **(a)** Sagittal T2-weighted MR image shows a 2.6 × 2 × 3-cm, ill-defined, intermediate-signal-intensity mass in the left vaginal vault. The patient previously underwent hysterectomy and bilateral salpingo-oophorectomy. **(b)** Axial T2-weighted MR image shows tumor extension to the paravaginal tissues. There is no invasion of the left levator sling, and the fat planes between the mass and the bladder and rectum are preserved.

mas, which appear as ill-defined heterogeneous-signal-intensity masses on T2-weighted MR images and low signal intensity on T1-weighted MR images (Fig 12). The vagina is one of the most common sites for recurrent endometrial cancer (53). This typically occurs at the vaginal vault. Vaginal metastases from uterine leiomyosarcomas and carcinosarcomas have a similar appearance to the primary tumor from which they have spread (37,51).

Ovarian cancer spread by peritoneal spread and involvement of the vagina occurs when disease invades from the peritoneal cavity into the vagina. This most commonly occurs at the vaginal vault (ie, at the pouch of Douglas) as this is the dependent part of the peritoneum, allowing tumor seeding to deposit. This occurs in primary and recurrent ovarian cancer. Involvement is best seen on sagittal T2-weighted images. A wide spectrum of histologic subtypes is recognized,

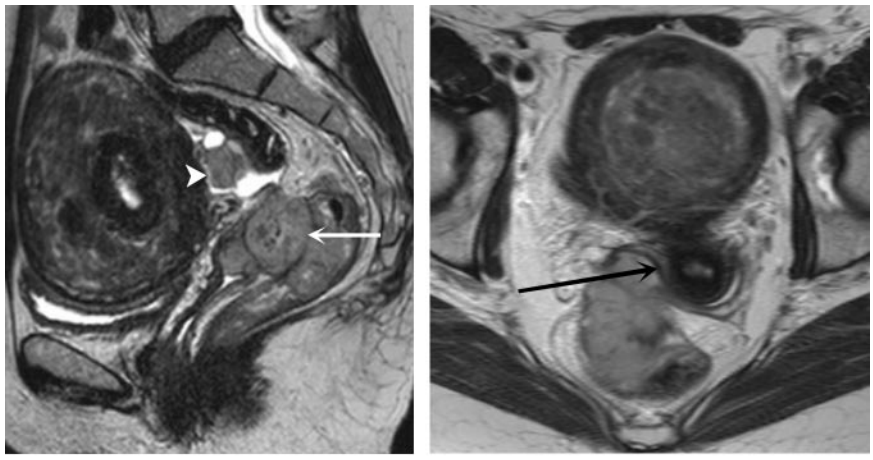

a. b.

Figure 13. Vaginal metastasis in a 54-year-old patient with stage IIIC ovarian adenocarcinoma and pelvic lymph node involvement who presented with a bulky rectovaginal mass. **(a)** Sagittal T2-weighted MR image shows a lobulated, 5.5 × 3.5-cm, homogeneous, intermediate-signal-intensity mass (arrow), which arises from the upper third of the vagina and invades the anterior wall of the rectum. There is a 3.3-cm right adnexal mass (arrowhead), which represents disease in the right ovary. There is also a bulky fibroid uterus. **(b)** Axial T2-weighted MR image shows that the vaginal mass arises from the right lateral and posterior walls of the fornix (arrow).

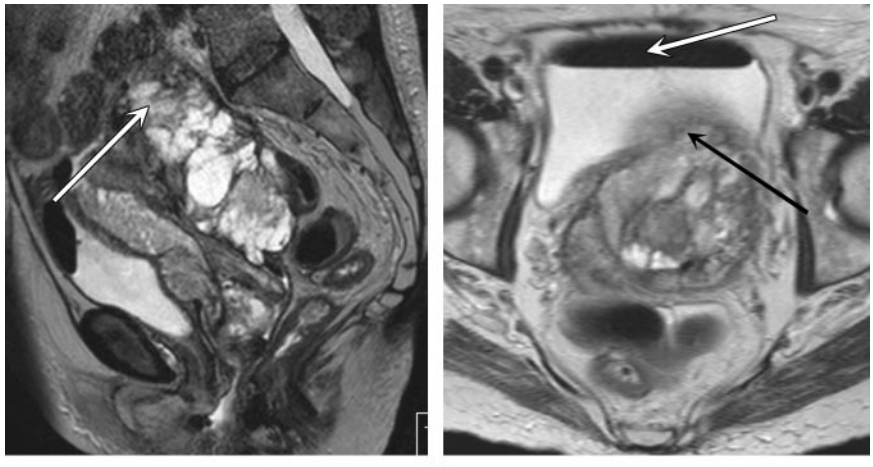

a. b.

Figure 14. Vaginal metastasis in a 60-year-old patient with a stage IIIC malignant ovarian mixed müllerian tumor who presented with vaginal bleeding, pneumaturia, and fecal leakage. **(a)** Sagittal T2-weighted MR image shows a 10 × 10 × 8.5-cm mass arising from the posterior vaginal vault and invading the sigmoid colon superiorly (arrow). The mass has heterogeneous high signal intensity and contains multiple loculi. **(b)** Axial T2-weighted MR image shows that the mass invades the bladder (black arrow), which contains gas (white arrow) as a result of a fistulous connection.

which are reflected in the MR imaging appearances (Figs 13–15) (54).

In patients who have undergone hysterectomy as part of treatment for their gynecologic malignancy, it is not possible at MR imaging to distinguish between a vaginal metastasis from the original primary (ie, cervical, uterine, or ovarian cancer) and a new primary vaginal carcinoma (55). In such cases, careful review of the clinical history or pathologic findings is required. MR imaging may be used to define the extent of vaginal involvement.

Metastases from Nongynecologic Malignancies

Rectal and bladder cancer may involve the vagina in advanced disease or if there is local relapse af-

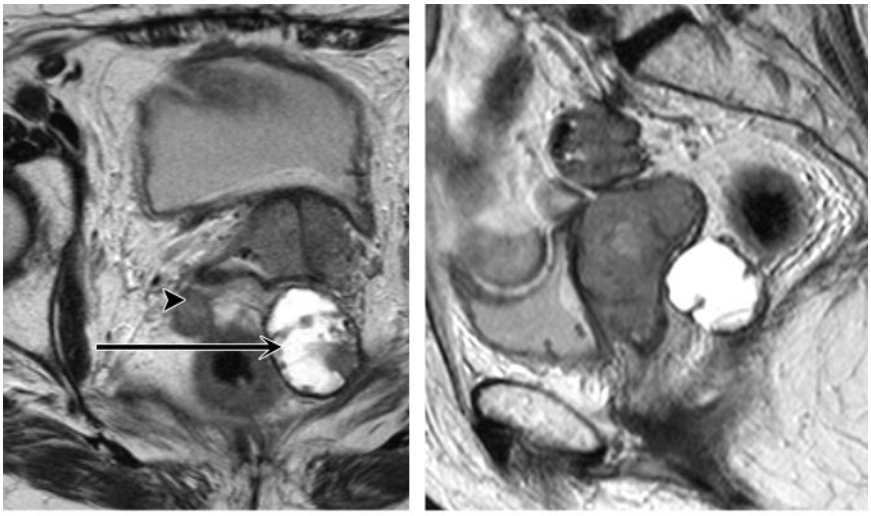

a. b.

Figure 15. Vaginal metastasis in a 67-year-old patient with stage IIIC ovarian serous cystadenocarcinoma who presented with intermittent bowel obstruction and vaginal discharge. **(a)** Axial T2-weighted MR image shows a 5-cm intermediate-signal-intensity mass that arises from the left lateral wall of the upper third of the vagina and indents the posterior wall of the bladder. The mass has a cystic component (arrow), which lies adjacent to the rectum and causes a bulge on the left levator sling. There is a satellite tumor nodule in the mesorectum (arrowhead). **(b)** Sagittal T2-weighted MR image shows the mass invading the lower rectum.

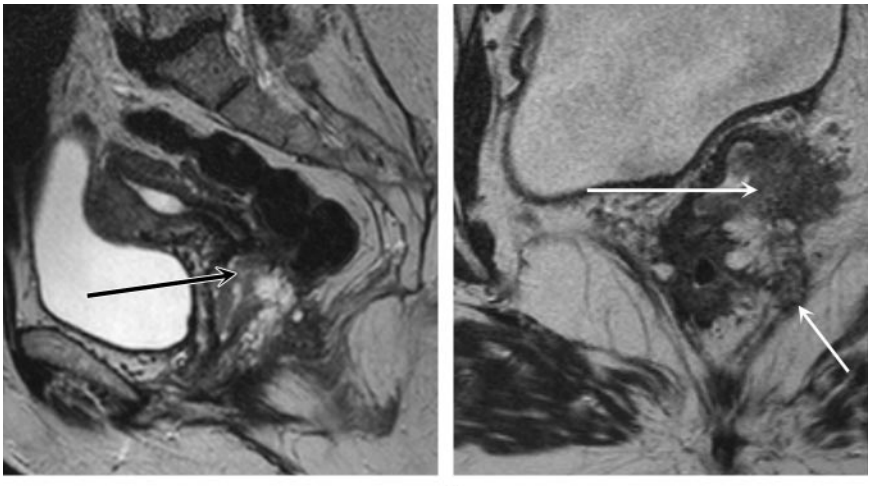

a. b.

Figure 16. Vaginal metastasis from rectal adenocarcinoma in a 59-year-old patient with a vaginal mass. The patient had a history of Dukes stage C rectal adenocarcinoma treated with a low anterior resection. **(a)** Sagittal T2-weighted MR image shows an irregular mass of intermediate to high signal intensity invading the posterior vaginal vault (arrow). **(b)** Axial T2-weighted MR image shows the infiltrative, irregular, 3.2 × 4-cm, intermediate- to high-signal-intensity mass arising from the left pararectal tissues and extending to the posterior vaginal vault (long arrow). The mass extends to the left levator sling (short arrow) and parametrium.

ter treatment. The imaging appearance reflects that of the local tumor. In rectal adenocarcinomas, vaginal involvement appears as fairly well-defined heterogeneous intermediate- to high-signal-intensity masses at T2-weighted MR imaging, depending on their mucinous content (Fig 16), and as homogeneously low-signal-intensity masses at T1-weighted MR imaging (51). Metastases from extragenital cancers are rare and most commonly occur from adenocarcinoma of the colon and breast (15), with colonic metastases reported to appear as high-signal-intensity masses, similar to adenocarcinoma of the colon.

There are a handful of case reports in the literature of metastases to the vagina from malignant melanoma. MR imaging features of these vaginal metastases vary depending on the melanin content of the metastases, a feature common to the primary tumor and also similar to primary vaginal melanoma (39).

Conclusions

The superb soft-tissue contrast resolution of MR imaging depicts the nature of vaginal malignancies. MR imaging allows detailed assessment of the anatomic extent of the disease and also its characteristic appearance, thus assisting in management of the tumor.

Acknowledgment: Our sincere thanks to Janet MacDonald for her help with obtaining the images used for publication.

References

1. Hatch KD, Fu YS. Cervical and vaginal cancer. In: Berek JS, Adashi EY, Hillard PA, eds. Novak's textbook of gynecology. 12th ed. Baltimore, Md: Williams & Wilkins, 1996; 1111–1153.
2. Chagpar A, Kanthan SC. Vaginal metastasis of colon cancer. Am Surg 2001;67:171–172.
3. Kim SH, Choi BI, Han JK, et al. Pre operative staging of uterine cervical carcinoma: comparison of CT and MRI in 99 patients. J Comput Assist Tomogr 1993;17:633–640.
4. Morgan MA, Mikuta JJ. Surgical management of vulvar cancer. Semin Surg Oncol 1999;17:168–172.
5. Schmidt WA. Pathology of the vagina. In: Fox H, Wells M, eds. Haines and Taylor obstetrical and gynecological pathology. 4th ed. Edinburgh, Scotland: Churchill-Livingstone, 1995; 176–180.
6. Dixit S, Singhal S, Baboo HA. Squamous cell carcinoma of the vagina: a review of 70 cases. Gynecol Oncol 1993;48:80–87.
7. Crum CP. The female genital tract. In: Kumar V, Abbas A, Fausto N, eds. Robbins and Cotran pathologic basis of disease. 7th ed. Philadelphia, Pa: Saunders, 2004; 1059–1118.
8. Al-Kurdi M, Monaghan JM. Thirty-two years experience in management of primary tumours of the vagina. Br J Obstet Gynaecol 1981;88:1145–1150.
9. Hawnaur J. Uterine and cervical tumours. In: Husband JE, Reznek RH, eds. Imaging in oncology. 2nd ed. London, England: Taylor & Francis, 2004; 467–496.
10. Chang YC, Hricak H, Thurnher S, Lacey CG. Vagina: evaluation with MR imaging. II. Neoplasms. Radiology 1988;169:175–179.
11. Siegelman ES, Outwater EK, Banner MP, Ramchandi P, Anderson TL, Schnall MD. High resolution MR imaging of the vagina. RadioGraphics 1997;17:1183–1203.
12. Chang SD. Imaging of the vagina. Radiol Clin North Am 2002;40:637–658.
13. Merino MJ. Vaginal cancer: the role of infectious and environmental factors. Am J Obstet Gynecol 1991;165(4 pt 2):1255–1263.
14. Togashi K, Konishi J. Magnetic resonance imaging in the evaluation of gynecologic malignancy. Magn Reson Q 1990;6:250–275.
15. Lindeque BG. The role of surgery in the management of carcinoma of the vagina. Baillieres Clin Obstet Gynaecol 1987;1:319–329.
16. Hellman K, Lundell M, Silfversward C, Nilsson B, Hellstrom AC, Frankendal B. Clinical and histopathological factors related to prognosis in primary squamous cell carcinoma of the vagina. Int J Gynecol Cancer 2006;16:1201–1211.
17. Perez CA, Grigsby PW, Garipagaoulu M, Mutch DG, Lockett MA. Factors affecting long term outcome of irradiation in carcinoma of the vagina. Int J Radiat Oncol Biol Phys 1999;44:37–45.
18. Hellman K, Silfversward C, Nilsson B, Hellstrom AC, Frankendal B, Petterson F. Primary carcinoma of the vagina: factors influencing the age at diagnosis—the Radiumhemmet series 1956–96. Int J Gynecol Cancer 2004;14:491–501.
19. Randall ME, Andersen WA, Mills SE, Kim JA. Papillary squamous cell carcinoma of the uterine cervix: a clinicopathologic study of nine cases. Int J Gynecol Pathol 1986;5:1–10.
20. Fetissof F, Haillot O, Lanson Y, Arbeille B, Lansac J. Papillary tumour of the vagina resembling transitional cell carcinoma. Pathol Res Pract 1990;186:358–364.
21. Carrington BM, Hricak H. The uterus and vagina. In: Hricak H, Carrington BM, eds. MRI of the pelvis: a text atlas. Norwalk, Conn: Appleton & Lange, 1991; 93–184.
22. Hricak H, Secaf E, Buckley DW, Brown JJ, Tanangho EA, McAninch JW. Female urethra: MR imaging. Radiology 1991;178:527–535.
23. Tsuda K, Murakami T, Kurachi H, et al. MR imaging of non-squamous vaginal tumors. Eur Radiol 1999;9:1214–1218.
24. Olson MC, Posniak HV, Tempany CM, Dudiak CM. MR imaging of the female pelvic region. RadioGraphics 1992;12:445–465.
25. Gilles R, Michel G, Chancelier MD, Vanel D, Masselot J. Case report: clear cell adenocarcinoma of the vagina—MR features. Br J Radiol 1993;66:168–170.

26. Haskel S, Chen SS, Spiegel G. Vaginal endometrioid adenocarcinoma arising in vaginal endometriosis: a case report and literature review. Gynecol Oncol 1989;34:232–236.
27. Morrow CP, Curtin JP. Tumors of the vagina. In: Synopsis of gynecological oncology. 5th ed. Philadelphia, Pa: Churchill Livingstone, 1998; 89–105.
28. Blythe JG, Michael H, Hodel KA. Colposcopic and pathologic features in two cases of DES-related vaginal clear cell carcinoma. J Reprod Med 1983;28:137–146.
29. Robboy SJ, Scully RE, Welch WR, Herbst AL. Intrauterine diethylstilbestrol exposure and its consequences: pathologic characteristics of vaginal adenosis, clear cell carcinoma and related lesions. Arch Pathol Lab Med 1977;101:1–5.
30. Donnelly LF, Gylys-Morin VM, Warner BW, Hillard PJA. Case report: clear cell adenocarcinoma of the vagina in a 5 year old girl—imaging findings. Clin Radiol 1998;53:69–72.
31. Chung AF, Casey MJ, Flannery JT, Woodruff JM, Lewis JL Jr. Malignant melanoma of the vagina: report of 19 cases. Obstet Gynecol 1980;55:720–727.
32. Moon WK, Kim SH, Han MC. MR findings of malignant melanoma of the vagina. Clin Radiol 1993;48:326–328.
33. Gupta D, Neto AG, Deavers MT, Silva EG, Malpica A. Metastatic melanoma to the vagina: clinicopathologic and immunohistochemical study of three cases and literature review. Int J Gynecol Pathol 2003;22:136–140.
34. Fan SF, Gu WZ, Zhang JM. Case report: MR findings of malignant melanoma of the vagina. Br J Radiol 2001;74:445–447.
35. Woodruff WW Jr, Djang WT, McLendon RE, Heinz ER, Voorhees DR. Intracerebral malignant melanoma: high-field-strength MR imaging. Radiology 1987;165:209–213.
36. Kim H, Jung SE, Lee EH, Kang SW. Magnetic resonance imaging of vaginal malignant melanoma. J Comput Assist Tomogr 2003;27:357–360.
37. Cantisani V, Mortele KJ, Kalantari BN, Glickman JN, Tempany C, Silverman SG. Vaginal metastasis from uterine leiomyosarcoma: magnetic resonance imaging features with pathological correlation. J Comput Assist Tomogr 2003;27:805–809.
38. Yoshizako T, Sugimura K, Kaji Y, Isohara M, Kitao M. Malignant vaginal melanoma: usefulness of fat-saturation MRI. Clin Imaging 1996;20:137–139.
39. Tavassoli FA, Norris HJ. Smooth muscle tumors of the vagina. Obstet Gynecol 1979;53:689–693.
40. Peters WA 3rd, Kumar NB, Andersen WA, Morley GW. Primary sarcoma of the adult vagina: a clinicopathologic study. Obstet Gynecol 1985;65:699–704.
41. Sahdev A, Sohaib SA, Jacobs I, Shepherd JH, Oram DH, Reznek RH. MR imaging of uterine sarcomas. AJR Am J Roentgenol 2001;177:1307–1311.
42. Shadbolt CL, Coakley FV, Qayyum A, Donat SM. MRI of vaginal leiomyomas. J Comput Assist Tomogr 2001;25:355–357.
43. O'Brien JM, Brennan DD, Taylor DH, et al. Skeletal muscle metastasis from uterine leiomyosarcoma. Skeletal Radiol 2004;33:655–659.
44. Schiffman R, Chong TW. Vaginal bleeding as a presenting symptom of synovial sarcoma. Cancer 1980;45:2428–2433.
45. Okagaki T, Ishida T, Hilgers RD. A malignant tumour of the vagina resembling synovial sarcoma: a light and electron microscope study. Cancer 1976;37:2306–2320.
46. McCarville MB, Spunt SL, Skapek SX, Pappo AS. Synovial sarcoma in pediatric patients. AJR Am J Roentgenol 2002;179:797–801.
47. Morton MJ, Berquist TH, McLeod RA, Unni KK, Sim FH. MR imaging of synovial sarcoma. AJR Am J Roentgenol 1991;156:337–340.
48. McNicholas MM, Fennelly JJ, MacErlaine DP. Imaging of primary vaginal lymphoma. Clin Radiol 1994;49:130–132.
49. Kim SH, Choi BI, Han MC, Kim YI. Retroperitoneal neurilemoma: CT and MR findings. AJR Am J Roentgenol 1992;159:1023–1026.
50. Siu SS, Lo KW, Chan AB, Yu MY, Cheung TH. Nodal detection in malignant melanoma using laparoscopic ultrasonography. Gynecol Oncol 2004;92:985–988.
51. Eisenberg LB, Semelka RC, Firat Z. Female urethra and vagina. In: Semelka RC, ed. Abdominal pelvic MRI. 2nd ed. Hoboken, NJ: Wiley, 2006; 1219–1247.
52. Outwater EK. CT and MRI of neoplasms metastatic to the genital tract. In: Anderson JC, ed. Gynaecologic imaging. London, England: Churchill Livingstone, 1999; 519–534.
53. Sohaib SA, Houghton SL, Meroni R, Rockall AG, Blake P, Reznek RH. Recurrent endometrial cancer: patterns of recurrent disease and assessment of prognosis. Clin Radiol 2007;62:28–34.
54. Brown MA, Ascher SM, Semelka RC. Adnexa. In: Semelka RC, ed. Abdominal pelvic MRI. 2nd ed. Hoboken, NJ: Wiley, 2006; 1333–1382.
55. Brown MA, Kubik-Huch RA, Reinhold C, Semelka RC. Uterus and cervix. In: Semelka RC, ed. Abdominal pelvic MRI. 2nd ed. Hoboken, NJ: Wiley, 2006; 1251–1331.

This article meets the criteria for 1.0 credit hour in category 1 of the AMA Physician's Recognition Award. To obtain credit, see accompanying test at http://www.rsna.org/education/rg_cme.html.

RadioGraphics

MR Imaging Features of Vaginal Malignancies

Jyoti H. Parikh, FRCR, et al

RadioGraphics 2008; 28:49–63 • **Published online** 10.1148/rg.281075065 • **Content Codes:** GU MR OB OI

Page 50
Malignant involvement of the vagina occurs more commonly from metastatic spread, and except for isolated reports of metastases from extragenital cancers (2), the most common cause of metastatic disease is direct local invasion from the female urogenital tract.

Page 50
MR imaging is crucial in demonstrating the location of the tumor, parametrial extension, pelvic sidewall involvement, and spread to the bladder or urethra, rectum, and lymph nodes. Furthermore, MR imaging can be of value in depicting pelvic anatomy for surgical and radiation therapy planning.

Page 50
These sequences are supplemented with high-resolution oblique axial (ie, perpendicular to the long axis of the vagina) T2-weighted fast spin-echo imaging (11). This sequence allows detailed assessment of the vaginal tumor and its relation to the paravaginal tissues and thus accurately demonstrates the extent of disease. Vaginal tumors are almost always best seen with this sequence.

Page 57
The lymph node drainage pattern of the vagina is such that lesions of the upper and middle thirds drain to the pelvic obturator nodes, internal and external iliac nodes, and paraaortic nodes and lesions of the lower third drain to the inguinal nodes. Posterior wall lymphatics communicate with rectal lymphatics and drain to the inferior gluteal, sacral, and rectal nodes.

Page 58
As a general rule, the MR imaging features of metastases to the vagina mimic the MR imaging features of the primary tumor, and T2-weighted MR imaging best delineates the extent of disease within and beyond the vagina.